K-shell resonant transfer and excitation in calcium ions

N. R. Badnell

Department of Physics, Auburn University, Auburn, Alabama 36849-5311
(Received 12 December 1989)

We have calculated K-shell cross sections for the process of resonant transfer excitation followed by x-ray stabilization (RTEX) in collisions of Ca^{q+} ($q = 10$–$12,16$–19) ions with H_2. Our KLn intermediate-coupling results are in excellent agreement with the experimental results of Tanis *et al.* [Phys. Rev. A **34**, 2534 (1986)] for $q = 16$–18, particularly when supplemented by our LS-coupling results for the KMn transitions. The comparison for $q = 19$ is hampered by the non-resonant background, but our results are consistent with experiment. Our LS-coupling results for KLn-plus-KMn transitions are in good agreement with experiment for $q = 11$ and 12. But for $q = 10$ our KMn RTEX cross sections are much smaller than the sparse experimental results, indicating a large nonresonant experimental background.

I. INTRODUCTION

Resonant transfer and excitation followed by x-ray stabilization (RTEX) in atom-ion collisions is the subject of much interest for the information it provides on dielectronic recombination (DR) in highly charged ions. In particular, RTEX has been studied extensively for the Li-like isoelectronic sequence (see Ref. 1 and references therein). It is now of interest to study isonuclear sequences, both to study the overall agreement between theory and experiment for RTEX and DR and to track other possible transfer excitation mechanisms.[2] Recently,[3] we have calculated L-shell RTEX cross sections for niobium ions ($q = 28$–32) and found mixed agreement with the experimental results of Bernstein *et al.*[4] We did, however, find that contributions from LMn, LNn, LOn, etc. RTEX transitions gave rise to good agreement with experiment in the high-energy tail for Nb^{31+}. This implied that only a small contribution was possible from the uncorrelated process[2] (UTEX).

In this paper we look at K-shell RTEX in calcium ions ranging from H-like ($q = 19$) to Ne-like ($q = 10$). Experimental results, due to Tanis *et al.*,[5] exist for collisions of Ca^{q+} ($q = 10$–$12,16$–19) ions with H_2. We have already noted[1] the importance of using intermediate coupling for Ca^{17+} and expect that the same will also be true for $q = 16$ and 18. For $q = 10$–12, Omar and Hahn[6] looked at peak cross-section ratios for different charge states using an angular-momentum-average scheme. We will use LS coupling; intermediate-coupling effects are usually small for more complex ions where there is more opportunity for LS-allowed mixing. Even so, due to the large number of terms arising from configurations with four open subshells, some transitions will still have to be neglected. The theory behind the calculations is outlined in Sec. II and the application to calcium ions is detailed in Sec. III. We present our results in Sec. IV and compare them with experiment. A summary is then given in Sec. V.

II. THEORY

Using the impulse approximation,[7] the total RTEX cross section $\sigma_x(i;\text{tot})$ for an initial state i may be written in terms of energy-averaged DR cross sections $\bar{\sigma}_d(i;j)$, thus

$$\sigma_x(i;\text{tot}) = \sum_j J(Q)\bar{\sigma}_d(i;j)\frac{\Delta E_c}{2I}\left[\frac{MI}{E}\right]^{1/2}. \quad (1)$$

$J(Q)$ is the Compton profile of the target gas with Q given by

$$Q = \frac{1}{2I}\left[E_c + E_t - \frac{Em}{M}\right]\left[\frac{MI}{E}\right]^{1/2}, \quad (2)$$

E is the projectile-ion energy in the laboratory frame, E_c is the $j \rightarrow i$ Auger energy, and E_t is the binding energy of the target electron, both in the rest frame of the projectile. M is the ionic mass, m the electron mass, and I is the ionization potential energy of hydrogen.

The energy-averaged DR cross section for a given initial state i through an intermediate state j is given by[8]

$$\bar{\sigma}_d(i;j) = \frac{(2\pi a_0 I)^2}{E_c \Delta E_c}\frac{\omega(j)}{2\omega(i)}$$
$$\times \frac{\tau_0 \sum_k A_r(j \rightarrow k) \sum_l A_a(j \rightarrow i, E_c l)}{\sum_h\left[A_r(j \rightarrow h) + \sum_l A_a(j \rightarrow h, E_c l)\right]}, \quad (3)$$

where $\omega(j)$ is the statistical weight of the $(N+1)$-electron doubly excited state, $\omega(i)$ is the statistical weight of the N-electron initial state, and $(2\pi a_0)^2\tau_0 = 2.6741 \times 10^{-32}$ cm^2 sec. Cascade is taken into account by restricting the sum over k to those states stable against autoionization, while the sum over h is over all possible states. A_a and A_r may then be evaluated in configuration-mixing LS-coupling and intermediate-coupling approximations using the AUTOSTRUCTURE package.[8,9]

III. APPLICATION TO CALCIUM IONS

We describe below the transitions that we consider for each calcium ion.

Ca^{19+}: We consider

$$1s + kl_c \rightleftarrows n_d l_d nl \rightarrow \begin{cases} 1snl + h\nu_1 \\ 1sn_d l_d + h\nu_2 \end{cases}$$
$$\downarrow$$
$$n'_d l'_d + kl'_c \, ,$$

where $l_c, l'_c = l, l\pm1$ for $n_d = 2$; $l_c, l'_c = l, l\pm1, l\pm2$ for $n_d = 3$ and $1 \le n'_d \le n_d$; $0 \le l_d < n_d$; $0 \le l'_d < n'_d$.

Ca^{18+}: We consider

$$1s^2 + kl_c \rightleftarrows 1sn_d l_d nl \rightarrow \begin{cases} 1s^2 nl + h\nu_1 \\ 1s^2 n_d l_d + h\nu_2 \end{cases}$$
$$\downarrow$$
$$1sn'_d l'_d + kl'_c \, ,$$

where $l_c, l'_c = l, l\pm1$ for $n_d = 2$; $l_c, l'_c = l, l\pm1, l\pm2$ for $n_d = 3$ and 4; and $1 \le n'_d \le n_d$; $0 \le l_d < n_d$; $0 \le l'_d < n'_d$.

Ca^{17+}: We consider

$$1s^2 2s + kl_c \rightleftarrows 1s2sn_d l_d nl \rightarrow \begin{cases} 1s^2 2snl + h\nu_1 \\ 1s^2 2sn_d l_d + h\nu_2 \end{cases}$$
$$\downarrow$$
$$\begin{cases} 1s2sn'_d l'_d + kl_{c'} \\ 1s^2 n_d l_d + kl''_c, & l''_c = l \\ 1s^2 nl + kl'''_c, & l'''_c = l_d \end{cases}$$

where $l_c, l'_c = l, l\pm1$ for $n_d = 2$; $l_c, l'_c = l, l\pm1, l\pm2$ for $n_d = 3$ and 4; and $1 \le n'_d \le n_d$; $0 \le l_d < n_d$; $0 \le l'_d < n'_d$.

Ca^{16+}: We consider

$$1s^2 2s^2 + kl_c \rightleftarrows 1s2s^2 n_d l_d nl \rightarrow \begin{cases} 1s^2 2s^2 nl + h\nu_1 \\ 1s^2 2s^2 n_d l_d + h\nu_2 \end{cases}$$
$$\downarrow$$
$$\begin{cases} 1s2s^2 n'_d l'_d + kl'_c \\ 1s^2 n_d l_d nl + kl''_c, & l''_c = 0 \\ 1s^2 2sn_d l_d + kl'''_c, & l'''_c = l \\ 1s^2 2snl + kl''''_c, & l''''_c = 0,1,2 \end{cases}$$

where $l_c, l'_c = l, l\pm1$ for $n_d = 2$; $l_c, l'_c = l, l\pm1, l\pm2$ for $n_d = 3$ and 4; and $1 \le n'_d \le n_d$; $0 \le l_d < n_d$; $0 \le l'_d < n'_d$.

Ca^{12+}: We consider

$$1s^2 2s^2 2p^4 + kl_c \rightleftarrows 1s2s^2 2p^5 nl \rightarrow \begin{cases} 1s^2 2s^2 2p^4 nl + h\nu_1 \\ 1s^2 2s^2 2p^5 + h\nu_2 \end{cases}$$
$$\downarrow$$
$$\begin{cases} 1s2s^2 2p^5 + kl'_c \\ 1s^2 2s2p^5 + kl'_c \\ 1s^2 2s^2 2p^3 nl + kl''_c, & l''_c = 0,2 \\ 1s^2 2s2p^4 nl + kl'''_c, & l'''_c = 1 \\ 1s^2 2p^5 nl + kl''_c, & l''_c = 0 \end{cases}$$

where $l_c = l\pm1$ and $l'_c = l$; and

$$1s^2 2s^2 2p^4 + kl_c \rightleftarrows 1s2s^2 2p^4 3pnl \rightarrow \begin{cases} 1s^2 2s^2 2p^4 3p + h\nu_1 \\ 1s^2 2s^2 2p^4 nl + h\nu_2 \end{cases}$$
$$\downarrow$$

$$\begin{cases} 1s2s^2 2p^5 + kl'_c \\ 1s^2 2s2p^4 nl + kl''_c, & l''_c = 1 \\ 1s^2 2s2p^4 3p + kl'''_c, & l'''_c = l \\ 1s^2 2s^2 2p^3 nl + kl''_c, & l''_c = 0,2 \\ 1s^2 2s^2 2p^3 3p + kl'''_c, & l'''_c = l\pm1 \\ \hline 1s^2 2p^4 3pnl + kl''_c, & l''_c = 0 \\ 1s^2 2s2p^3 3pnl + kl''_c, & l''_c = 1 \\ 1s^2 2s^2 2p^3 pnl + kl''_c, & l''_c = 0,2 \end{cases}$$

where $l_c = l\pm1$ and $l'_c = l, l\pm2$. In principle we should include all the listed autoionizing transitions but in practice the configurations below the line have to be omitted to render the problem tractable.

Ca^{11+}: We consider

$$1s^2 2s^2 2p^5 + kl_c \rightleftarrows 1s2s^2 2p^6 nl \rightarrow \begin{cases} 1s^2 2s^2 2p^5 nl + h\nu_1 \\ 1s^2 2s^2 2p^6 + h\nu_2 \end{cases}$$
$$\downarrow$$

$$\begin{cases} 1s^2 2s^2 2p^4 nl + kl'_c, & l'_c = 0,2 \\ 1s^2 2s2p^5 nl + kl'_c, & l'_c = 1 \\ 1s^2 2p^6 nl + kl'_c, & l'_c = 0 \\ 1s^2 2s2p^6 + kl'_c, & l'_c = l \\ 1s2s^2 2p^4 nl + kl'_c, & l'_c = 0,1,2,3 \end{cases}$$

where $l_c = l\pm1$; and

$$1s^2 2s^2 2p^5 + kl_c \rightleftarrows 1s2s^2 2p^5 3pnl \rightarrow \begin{cases} 1s^2 2s^2 2p^5 3p + h\nu_1 \\ 1s^2 2s^2 2p^5 nl + h\nu_2 \end{cases}$$
$$\downarrow$$

$$\begin{cases} 1s2s^2 2p^6 + kl'_c \\ 1s2s2p^5 nl + kl''_c, & l''_c = 1 \\ 1s^2 2s2p^5 3p + kl''_c, & l''_c = l \\ 1s^2 2s^2 2p^4 nl + kl''_c, & l''_c = 0,2 \\ 1s^2 2s^2 2p^4 3p + kl''_c, & l''_c = l\pm1 \\ \hline 1s^2 2p^5 3pnl + kl''_c, & l''_c = 0 \\ 1s^2 2s2p^4 3pnl + kl''_c, & l''_c = 1 \\ 1s^2 2s^2 2p^3 3pnl + kl''_c, & l''_c = 0,2 \end{cases}$$

where $l_c = l\pm1$ and $l'_c = l, l\pm2$. Again, we have omitted those configurations below the line.

Ca^{10+}: We consider

$$1s^22s^22p^6+kl_c \rightleftharpoons 1s^22s^22p^63l_d nl \rightarrow \begin{cases} 1s^22s^22p^63l_d+h\nu_1 \\ 1s^22s^22p^6nl+h\nu_2 \end{cases}$$

$$\downarrow$$

$$\begin{cases} 1s^22p^63l_d nl+kl_c', & l_c'=0 \\ 1s^22s^22p^5nl+kl_c', & l_c'=0,1,2,3 \\ 1s^22s2p^6nl+kl_c', & l_c'=0,1,2 \\ 1s^22s^22p^53l_d+kl_c', & l_c'=l\pm1 \\ 1s^22s2p^63l_d+kl_c', & l_c'=l \\ \hline 1s^22s^22p^43l_d nl+kl_c', & l_c'=0,2 \\ 1s^22s2p^53l_d nl+kl_c', & l_c'=1 \end{cases}$$

where $l_c=l,l\pm1,l\pm2$; $l_d=0,1,2$ and we have omitted the configurations below the line.

For Ca^{q+} ($q=10$–12) our *KMn* results represent an upper limit due to the neglect of certain autoionizing transitions.

IV. RESULTS

We present out results for *K*-shell RTEX cross sections for collisions of Ca^{q+} ($q=10$–$12,16$–19) ions with H$_2$ in Figs. 1–7 and compare them with the experimental results of Tanis et al.[5] The experimental error bars denote a maximum estimated[5] relative uncertainty of $\pm10\%$, while the estimated[5] absolute uncertainty is $\pm30\%$. The energy that we plot is that of the projectile ion in the laboratory frame times m/M; see Sec. II.

A. Ca^{19+}

The comparison of theoretical and experimental results for H-like calcium is complicated by the additional process of electron capture into an excited state by the projectile nucleus followed by the emission of a *K*-shell x ray.[5] We have added our theoretical RTEX results to those of the background process obtained by fitting to the experimental data both above and below the RTEX energy region. The net result (Fig. 1) is consistent with exper-
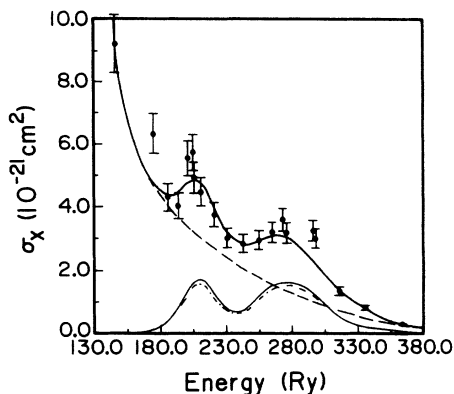

FIG. 1. *K*-shell RTEX cross sections for Ca^{19+}+H$_2$. ———, intermediate coupling both with and without the nonresonant experimental background; —·—·—·, *LS* coupling; — — —, fit to the experiment background of Tanis et al. (Ref. 5). ⊥, experimental points from Tanis et al. (Ref. 5).

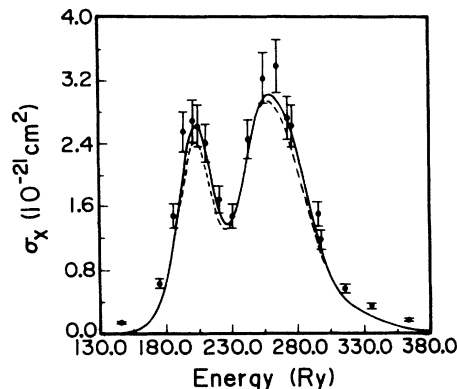FIG. 2. *K*-shell RTEX cross sections for Ca^{18+}+H$_2$. ———, intermediate coupling; — — —, *LS* coupling; both this work. ⊥, experimental points from Tanis et al. (Ref. 5).

iment. Also, there is little difference between our *LS*-coupling and intermediate-coupling results for the *KLn* transitions, while *KMn* transitions make only a small contribution in the high-energy tail.

B. Ca^{q+} ($q=16,17,18$)

For these three ions (Be-like, Li-like, and He-like) we have calculated RTEX cross sections for *KLn* transitions in both *LS*-coupling and intermediate-coupling schemes, while our results for *KMn* and *KNn* transitions have been calculated in *LS* coupling only. We have already noted[1] the importance of using intermediate coupling for Ca^{17+}. Similarly, our intermediate-coupling results for Ca^{16+} and Ca^{18+} (Figs. 2 and 4) are in better agreement with the experimental results of Tanis et al.[5] than our *LS*-coupling results. We also noted previously[1] for Ca^{17+} a discrepancy between theory and experiment over the position of the well-defined double peak structure. Our results for Ca^{16+} and Ca^{18+} show the same discrepancy. Consequently, we have lowered the experimental energies by 4 Ry (4 MeV in the laboratory frame) for all the ions. The second discrepancy noted in our work[1] on Ca^{17+} was in the high-energy tail. To this end we have now evaluated the contributions from *KMn* and *KNn* transitions, in *LS* coupling only. For all three ions this gives rise to a significant contribution in the high-energy tail (see Figs.
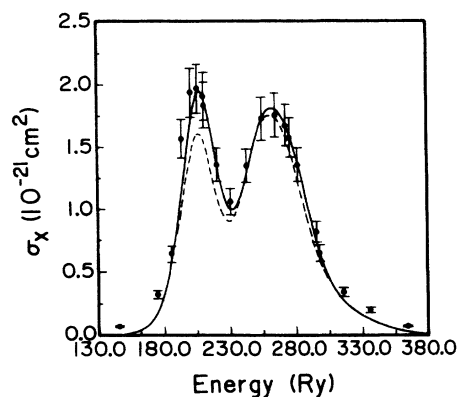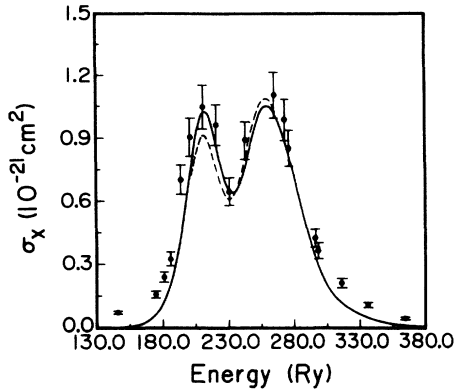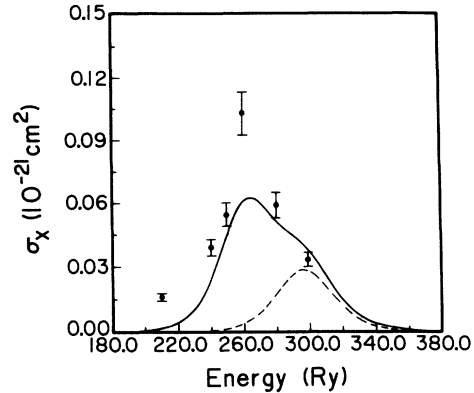

FIG. 3. As in Fig. 2, but for Ca^{17+}.

N. R. BADNELL

FIG. 4. As in Fig. 2, but for Ca^{16+}.

FIG. 6. As in Fig. 5, but for Ca^{11+}.

2–4) and is mainly due to KMn transitions. However, unlike our previous work[3] with Nb^{31+}, these higher RTEX transitions do not completely account for the high-energy tail of the experimental results. It is possible that electron capture by the projectile nucleus together with electronic excitation by a target gas electron, uncorrelated transfer and excitation UTEX,[2] could account for the remaining difference. We also note a small discrepancy between theory and experiment at low energies. This may be due to electron capture by the projectile nucleus together with electronic excitation by the target gas nucleus, nonresonant transfer and excitation NTEX.[2] Overall, however, there is excellent agreement between our intermediate-coupling RTEX results and experiment for Ca^{q+} ($q = 16-18$).

C. Ca^{q+} ($q = 10, 11, 12$)

For the previous ions the L shell was effectively empty as far as RTEX is concerned since it is dominated by $1s \rightarrow 2p$ core transitions. For these three ions (Ne-like, F-like, and O-like) the L shell is ($q = 10$) or is nearly ($q = 11,12$) filled. Thus the K-shell RTEX cross section is now much smaller and KMn transitions are of greater relative importance. In particular, for $q = 12$ (O-like) we see in Fig. 5 both the KLL peak at 230 Ry, the KLn

($n > L$) peak at 260 Ry, and the KMn peak at 300 Ry. For $q = 11$ (F-like) the KLL channel is closed and we are left with the KLn ($n > L$) and KMn peaks; see Fig. 6. Then for $q = 10$ (Ne-like) the KLn ($n > L$) channel is also closed and we are just left with the KMn peak; see Fig. 7. Our results for KLn and KMn transitions were evaluated in LS coupling only for these ions ($q = 10-12$) and our KMn results may be an overestimate due to the neglect of certain autoionizing transitions involving configurations with four open subshells; see Sec. III. However, for Ca^{12+} there is very good agreement between our theoretical results and the experimental results of Tanis et al.[5] (see Fig. 5) particularly in the energy region dominated by KMn transitions. Our results for Ca^{11+} are in fair agreement with the sparse experimental data (see Fig. 6), the one point at 260 Ry being the main discrepancy. Both for Ca^{11+} and Ca^{12+} there is still some experimental signal at energies below the theoretical RTEX contributions which could be due to NTEX. This is manifest for Ca^{10+} where the experimental results[5] have been attributed[10] to NTEX; see Fig. 7. For a Ne-like ion in the ground state there are no KLn transitions. The only RTEX signal is from KMn and higher transitions which peaks at 300 Ry according to theory. The experimental results (albeit only for three points) around 260 Ry cannot be accounted for by RTEX from the ground state in
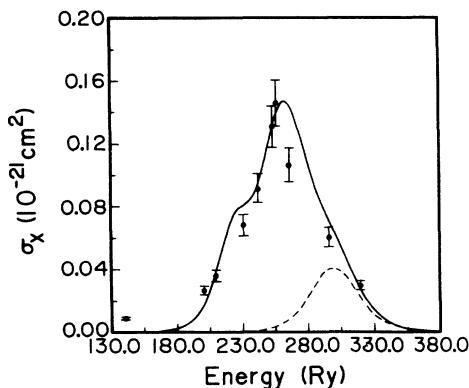

FIG. 5. K-shell RTEX cross sections for $Ca^{12+} + H_2$. ———, $KLn + KMn$ transitions; — — —, KMn transitions only; both LS coupling this work. ⟋, experimental points from Tanis et al. (Ref. 5).
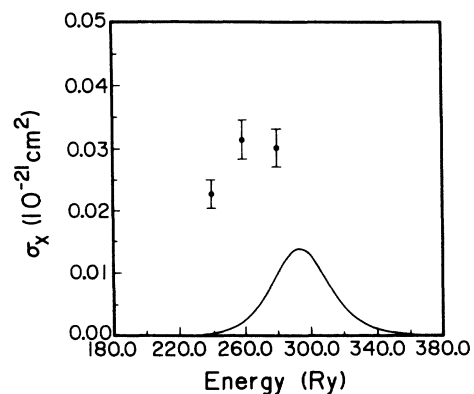

FIG. 7. K-shell RTEX cross sections for $Ca^{10+} + H_2$. ———, LS coupling; this work. ⟋, experimental points from Tanis et al. (Ref. 5).

theory. But *KLn* transitions do arise from the Ca^{10+} metastable $1s^2 2s^2 2p^5 3s\ {}^3P$. However, we have evaluated RTEX from this state and even for 100% occupation the result is negligible ($\sim 1 \times 10^{-24}$ cm^2). It would be useful to have experimental data over a wider range of energies for $q = 10$.

V. SUMMARY

We have calculated *K*-shell RTEX cross sections for collisions of Ca^{q+} ($q = 10-12, 16-19$) ions with H$_2$ and compared them with the experimental results of Tanis *et al.*[5] Our intermediate-coupling results are in excellent agreement with experiment for $q = 16-18$ and are a significant improvement over our *LS*-coupling results. There is a significant contribution from *KMn* transitions at high energies although some differences from experiment remain. Our results for $q = 19$ are consistent with experiment given that comparison is complicated by the one-electron nonresonant background. For $q = 10-12$ our results are an order of magnitude smaller than for $q = 16-19$ due to the increasing occupancy of the *L*-shell and *KMn* transitions are of greater relative importance. Our *LS*-coupling results are in good agreement with experiment for $q = 12$ while for $q = 11$ the experimental data is too sparse to tell if there is any real disagreement.

For $q = 10$ we obtain only a small contribution from RTEX at the experimental energies. For this case it appears then that the experimental cross sections are dominated by nonresonant transfer and excitation. It is desirable to have more experimental data for $q = 11$ and, in particular, $q = 10$.

VI. CONCLUSIONS

Overall, the agreement between theory and experiment is much better for *K*-shell RTEX than for *L*-shell. The agreement is such that it is possible to differentiate between results from different coupling schemes and to put limits on the small contributions from other transfer excitation mechanisms. RTEX is a useful source of experimental information on dielectronic recombination and is complementary to that from electron coolers and from ion traps.

[1]N. R. Badnell, Phys. Rev. A **40**, 3579 (1989).
[2]Y. Hahn, Phys. Rev. A **40**, 2950 (1989).
[3]N. R. Badnell, preceding paper, Phys. Rev. A **42**, 204 (1990).
[4]E. M. Bernstein, M. W. Clark, J. A. Tanis, W. T. Woodland, K. M. Berkner, A. S. Schlachter, J. W. Stearns, R. D. DuBois, W. G. Graham, T. J. Morgan, D. W. Meuller, and M. P. Stockli, Phys. Rev. A **40**, 4085 (1989).
[5]J. A. Tanis, E. M. Bernstein, M. W. Clark, W. G. Graham, R. H. McFarland, T. J. Morgan, J. R. Mowat, D. W. Meuller, A. Müller, M. P. Stockli, K. H. Berkner, P. Gohil, R. J. McDonald, A. S. Schlachter, and J. W. Stearns, Phys. Rev. A **34**, 2543 (1986).
[6]G. Omar and Y. Hahn, Phys. Rev. A **35**, 918 (1987).
[7]D. Brandt, Phys. Rev. A **27**, 1314 (1983).
[8]N. R. Badnell, J. Phys. B **19**, 3827 (1988).
[9]N. R. Badnell and M. S. Pindzola, Phys. Rev. A **39**, 1685 (1989).
[10]J. A. Tanis, Nucl. Instrum. Methods **A262**, 52 (1987).